

A MATHEMATICAL MODEL AND AN EXPERIMENTAL SETUP FOR THE RENDERING OF THE SKY SCENE IN A FOGGY DAY

SORIN CURILĂ¹, MIRCEA CURILĂ², DIANA CURILĂ (POPESCU)³, CRISTIAN GRAVA¹

Key words: Rendering, Foggy image, Scattering, Homogeneous and Heterogeneous fog.

The rendering of the scene under different atmospheric conditions requires the use of effects in the image, such as sunlight interaction with scene objects, suspended particles in the air, or shadows. In this paper, a mathematical model of the foggy image is analysed, the way aerosols modify the light in order to understand the resulting brightness of the scene captured by the camera. We calculate the intensity of scene radiation at the camera by taking into account the phenomena of scattering and absorption determined by the aerosols. Although most of the methods for rendering the sky scene in foggy conditions use the representation of a homogeneous fog, neglecting the heterogeneous fog, here both aspects are addressed. The heterogeneity is a consequence of a different number of dispersion particles appearing on the transmission directions of the scene radiation. The sky scene in a foggy day is rendered realistically in the experimental results section.

1. INTRODUCTION

The rendering of the virtual environment, an important component of the applications that use the augmented reality, requires the access to a large number of elements, such as sunlight, bluesky representation, fog, nature elements, the interaction between the sky and objects, etc. The radiance of objects due to sunlight is the most important source in the rendering of the sky scene. The shadows of the objects and the representation of the sky with a non-homogeneous aspect determined by clouds are effective elements to make the display as realistic as possible. At a small distance above the surface of the Earth, the atmosphere is composed of air molecules and a set of solid or liquid particles dispersed in a gaseous environment. These particles significantly influence the transfer of radiant energy in the atmosphere.

As Narasimhan and Nayar say in their work, the interaction of light with the atmosphere is investigated by atmospheric optics and the literature in this domain has been written over the past two centuries. But this research aims to find models of the atmosphere needed to implement the artificial vision. Narasimhan and Nayar [1] studied the visual manifestations of different weather conditions and modelled the chromatic effects of the atmospheric scattering. They derived geometric constraints on the scene and used them for computing artificial foggy image, depth segmentation, for extracting 3D structure and computing a clear scene.

The geometry of the imaging scene from the atmosphere was described by J.P. Oakley and B.L. Satherley [2]. They solve the problem of the foggy image enhancement by compensating for the attenuation and scattering of light.

Narendra Singh Pal et al. used for the foggy image the degradation model designed by Koschmieder [3]. Their framework for enhancing visibility applies a trilateral filter on observations to obtain the smooth fogless image, next, an S-shaped transfer mapping is used for contrast enhancement.

Fan Guo et al. propose a rendering method based on transmission map estimation using the Markov random field model and the bilateral filter [4]. Non-homogeneity in the transmission law is also taken into account. Artificial foggy images are rendered by generated 2D Perlin noise and the transmission map, according to the model of the atmospheric optics.

Xinhua Wang et al. present in their work a polarization image acquisition method based on the Stokes vectors [5].

They use an optical detection system composed of four polarizers with different polarization directions, whose final acquisition data is not affected by the presence of the scattering environment. The four Stokes parameters determine the non-degraded scene.

Anshu Kumari and Amarjeet Kumar Ghosh describe in their work [6] a method consisting of a colour optimization over a model of haze formation that finds the dehazed image and scaled depth of the scene, then proceed to an optimization using the Constraint of Constant Depth (CDC). The second stage determines the scattering coefficient that is strongly correlated to the levels of particulate matter.

Kenneth J. Voss and Stephanie Flora discuss in their work on the transmission coefficient used to propagate radiance in seawater, another scattering environment [8].

The scattering of light by liquid particles generates the gray veil of the fog and the scattering of light by the air molecules determines the blue sky. Because of the different types of interactions between molecules, particles, light and nature elements, it is not easy to obtain a mathematical model that describes the scene under different atmospheric conditions. Thus, in our work, we take into account the physics of light and particles, in particular the scattering and absorption during the transmission of radiation through the atmosphere.

Our contribution consists in treating both aspects for rendering the sky scene in foggy conditions: we take into account the homogeneous and the heterogeneous fog, without neglecting one of them as happens in most of the methods. Our practical and original experiments are mainly described in Section 5, Experimental results, and we also adapted and integrated some theoretical notions described in sections 3 and 4.

2. TRANSMISSION OF RADIATION THROUGH FOG

Here, we describe a method with a physical foundation to model the sky scene in conditions of a homogeneous foggy day. The radiative transfer through fog is expressed by Schwarzschild equation as follows:

$$dL_{\lambda} = -\beta_{\lambda}L_{\lambda}(z)dz + \beta_{\lambda}L_S dz, \quad (1)$$

¹ University of Oradea, Romania, Electronics and Telecommunications Department, 1 Universităţii Street, Oradea, 410087, Romania, E-Mail: sorincurila2015@yahoo.com

² University of Oradea, Romania, Environmental Engineering Department

³ University of Oradea, Romania, Mathematics and Computer Science Department

where $L_\lambda(z)$ is the intensity of radiation passing through the dispersive environment of thickness z , β_λ is the extinction

coefficient related to the visibility distance (which depends on the wavelength) and L_S is the sunlight intensity.

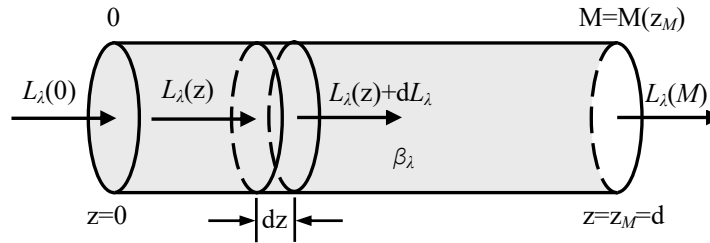


Fig. 1 – Direct transmission path between $z = 0$ and M point.

Assuming

a collimated beam of light with a unitary cross-section traversing the dispersive environment of thickness dz , the fractional change in intensity of radiation is the first term of eq. (1). This term expresses a relationship between the light intensity and the properties of the dispersive environment. Part of the radiance of the scene is scattered in a different direction from that of the direct transmission

path and is absorbed into the atmosphere as molecular energy, rotations and vibrations.

The thickness of the direct transmission path between z and M point (Fig. 1) is given by the following expression:

$$t_\lambda(z) = \int_z^M \beta_\lambda dz = \beta_\lambda(z_M - z). \quad (2)$$

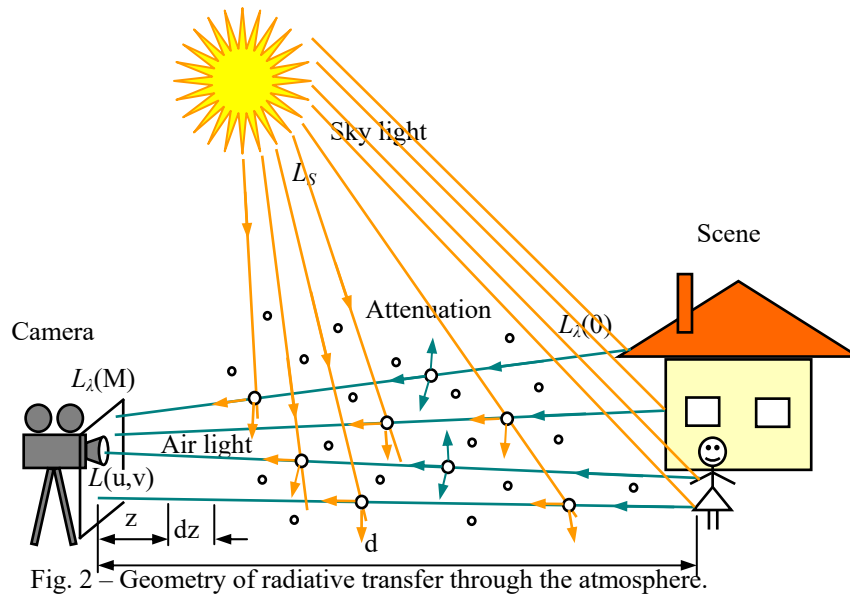


Fig. 2 – Geometry of radiative transfer through the atmosphere.

As the geometry of the radiative transfer shows, the sunlight is scattered in all possible directions. Part of the scattered light reaches the direct transmission path and picks up the intensity value of the pixel captured by the camera [2].

According to Fig. 2, if an increase ($z, z + dz$) of the direct transmission path is considered, the fractional change of radiation intensity because of the scattering of sunlight can be expressed as follows:

$$dL_\lambda = \beta_\lambda L_S dz. \quad (3)$$

This term, the second one of the eq. (1), describes the emission of thermal radiation on the direct transmission path. It is commonly referred to as airlight. The negative sign in eq. (1) suggests that the intensity value goes down as the thickness of the direct transmission path increases, while the positive sign expresses a pickup in the intensity value as the mentioned thickness increases.

Here, we propose a mathematical model of the homogeneous foggy image, taking into account the above consideration. The algorithm used to obtain the proposed model can be described using the following pseudo-code:

- start from the relation between the skylight intensity L_S and the intensity of radiation passing through the dispersive environment of thickness z , L_λ ;
- rewriting the expression of the skylight and environment intensities depending on the thickness of the direct transmission path between z and M point, $t_i(z)$;
- differentiation depending on $t_i(z)$;
- integration between $[0, M]$, depending on $t_i(z)$;
- computation of the intensity of radiation passing through the dispersive environment of thickness z , L_λ .

Using the above described algorithm, we obtain the following expression of L_λ :

$$L_\lambda(M) = L_\lambda(0)e^{-\beta_\lambda d} + L_S(1 - e^{-\beta_\lambda d}). \quad (4)$$

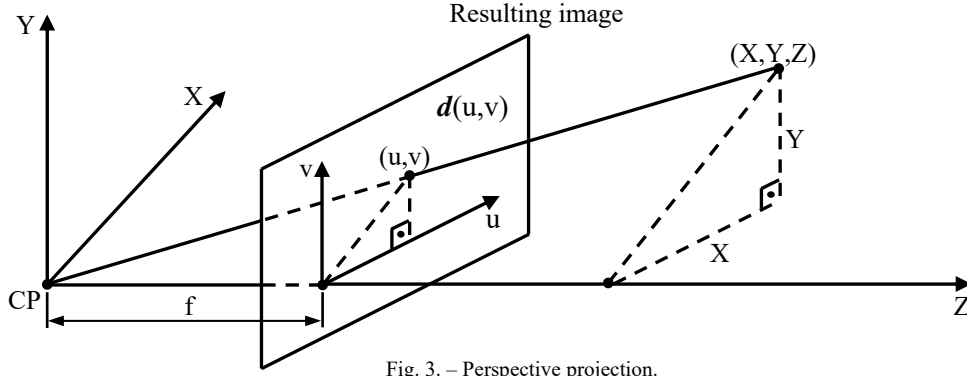


Fig. 3. – Perspective projection.

The last equation gives us the mathematical model of the homogeneous foggy image which expresses the attenuation of object radiance and the overlap of atmospheric veil $L_S(1 - e^{-\beta_\lambda d})$, where $L_\lambda(M(u, v))$ is the intensity of the captured pixel, $L_\lambda(0)$ is the intensity of the scene radiance, β_λ is the extinction coefficient of the atmosphere, $\mathbf{d}(u, v)$ is the distance map between the scene and the camera and L_S is the skylight intensity. As it will be shown, this mathematical model can be extended to implement both aspects of the fog, homogeneous and heterogeneous.

3. DISTANCE MAP

In other words, the distance map represents the matrix of all distances between the camera image and the corresponding points on the objects from the scene. In this paper, we have at our disposal the distance map $\mathbf{d}(u, v)$ necessary for the equation (4) to simulate the image in foggy conditions. This was generated by using approximate measurements and the perspective projection system.

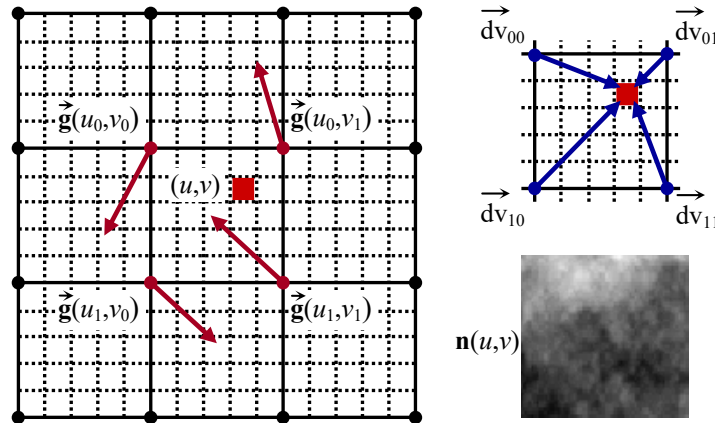


Fig. 4 – Grid, gradient vectors and distance vectors, Perlin noise.

We present the perspective projection subject under the following hypotheses: the centre of projection CP is the origin of the Cartesian coordinate system that describes problems in our surrounding space and the resulting image is in front of CP.

By applying the similarity of triangles in Fig. 3, we deduce:

$$u = \frac{fX}{Z}, v = \frac{fY}{Z}, Z(u, v) = f \quad (5)$$

where f is the focal length. It is the division by Z that produces the dimension variations of the objects related to the distance to the projection centre CP.

Not all the depth indexes, that provide *information* about the structure of the *scene*, are kept exactly to design the pseudo distance map. Real effects are implemented by setting the distances on specific partitions, choosing the fog's type and the extinction coefficient of the atmosphere. The atmospheric veil can be applied specifically by suitably setting the distances. An illustration of the two distance maps $\mathbf{d}(u, v)$, generated with the mentioned method, can be found in Fig. 8 (Section 5).

A *smooth noise* is added to generate heterogeneous

fog.

4. MATHEMATICAL MODEL OF THE USED NOISE

Here we use Perlin noise. This one produces a smooth sequence of pseudo-random numbers, where the value of the noise increases or decreases gradually between two generated *gradient vectors*. The 2D algorithm generates a texture showing an atmospheric cloud. The basics of Perlin noise are presented by Matt Zucker [10].

The Perlin noise algorithm computes the noise function $\mathbf{n}(u, v)$ for each vector $\overline{(u, v)}$ of the input image. In the beginning, a grid is laid over the whole image (bolded lines to be considered from Fig. 4) and one computes the coordinates (u_0, v_0) , (u_1, v_0) , (u_0, v_1) , (u_1, v_1) of the cell where is the vector $\overline{(u, v)}$. The details from the final image are controlled by changing the dimension of the grid.



Fig. 5 – a), d) Images in good weather conditions; c) image with modified brightness; b), e) images in foggy conditions.

We generate one random vector at a time, $\vec{g}(u_0, v_0)$, $\vec{g}(u_1, v_0)$, $\vec{g}(u_0, v_1)$ and $\vec{g}(u_1, v_1)$, called *gradient vectors*, using the Matlab function *randn*([,]), for the four points that delimit the cell. For the next step, we need to compute the *distance vectors* that have their tails in the points that mark the limit of the cell and their heads in the point where we compute the noise function:

$$\vec{d}_{ij} = \overline{(u, v)} - \overline{(u_i, v_j)} \quad i, j \in \{0, 1\}, \quad (6)$$

Next, we calculate the dot product between the gradient and distance vectors with respect to each point from the interior of the cell, that we denote dp_{00} , dp_{01} , dp_{10} and dp_{11} .

Thus, we compute dp_{00} , dp_{01} , dp_{10} and dp_{11} numbers by input vector $\overline{(u, v)}$ and the mentioned random generator function.

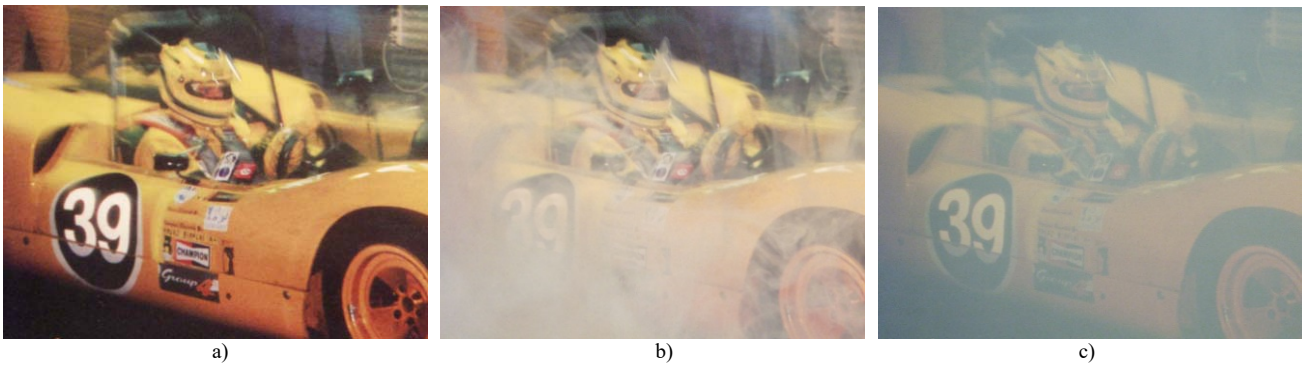


Fig. 6 – a) Original image; b) heterogeneous dispersive medium; c) homogeneous dispersive medium.

We will interpolate the result of the scalar products by using two-dimensional linear interpolation to get the final value, at that point, of noise function $\mathbf{n}(u, v)$.

5. EXPERIMENTAL RESULTS

At the beginning of this section, we present the first step made to undertake “the rendering of the sky scene in a foggy day”, that consisted of capturing images under good weather conditions and then in foggy conditions of exterior building). The obtained results are illustrated in Fig. 5.

Thereby, the nearby objects look clearly in the foggy condition images (see the tree from Fig. 5 b) or the two door pillars from Fig. 5 e)), while far objects become more and more faded until they fade away in the background.

As an example, consider the red building in Fig. 5 e), then the bridge and the far buildings beyond it. These

characteristics are absent in the image from Fig. 5 c), which was obtained from the original image from Fig. 5 a) to which we modified the brightness by adding a constant value to the three RGB components.

Next, we describe a physics experiment through which we aim to highlight the presence of the dispersion medium during the time of taking photos (the homogeneous, respectively the heterogeneous one). Thus, we used a glass aquarium filled with clean water. On one of its walls, we glued a poster with a picture of a pilot in the race car. The lighting conditions are those in the laboratory with midday natural light. After we placed the camera in front of the aquarium, fixed on a tripod (close to the wall opposite the one on which we placed the photo), we took the first photo, the original one (the photo from Fig. 6. a) without the light scattering).



Fig. 7 – a, d) Images with simulated fog-homogenous dispersion medium (β_λ); c) image in good weather conditions; b), e) images with simulated fog-heterogeneous dispersion medium, $\beta'_\lambda(u, v)$.

Then, we poured the content of a cup of milk in the water-filled aquarium. At this stage the mixture was

heterogeneous. We quickly took some photos, of which we present one in Fig. 6. b).

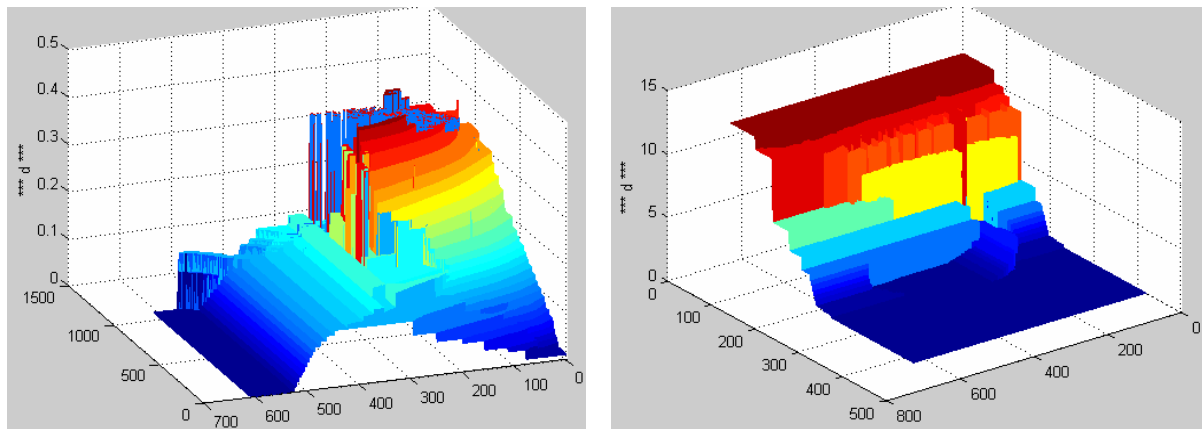


Fig. 8 – Distance maps for a) 5 bridge image and c) 7 ship image.

Then, with a glass rod, we mixed it to obtain the characteristics of a homogeneous environment and we again took some photos of which we present one in Fig. 6 c). In these two cases, the distance between the scene and the camera is constant. As it can be seen, the presence of the dispersion medium during photo shooting generates an effect similar to the real fog. For the most part, the difference is due to the constant distance between the scene and the camera. In the case of the described experiment, the dispersion environment is the water (and not the air as in the case of real fog) and the dispersive medium is done by the particles suspended in milk (and not the aerosols in the case of real fog).

In Fig. 7 we present the results of the simulation of the fog using eqs. (4), (7). The images show the characteristics mentioned above: clarity for the nearby objects (see the tree on the right and the first part of the road in Figs. 7 a, b, the

ship, the boat and the sea in Figs. 7 d, e), while the distant objects become blurred until they disappear in the background (see the bridges and distant buildings that are after them in the Figs. 7 a, b, d, e).

Often, the real fog presents some intense areas, others less intense, until the voids of the dispersion medium. The transition from one area to another is smooth. The heterogeneity is determined by the different number of particles (aerosols) on the radiation transmission directions. To model these characteristics, we introduce variability in the transmission law (4) by adding to the homogeneous dispersion coefficient β_λ a weighted value of the Perlin noise $\alpha * n(u, v)$ (weight required for dynamic adjustment).

$$\beta'_\lambda(u, v) = \beta_\lambda + \alpha * n(u, v). \quad (7)$$

6. CONCLUSIONS

This paper presents some of the steps that we have performed to display the fog weather phenomenon in images as realistic as possible. We put in place an experimental setup regarding the acquisition of the images in good weather conditions and during fog time, the physical experiment regarding the transmission of light through a dispersive environment, the analysis of the fog characteristics, the approach of the model regarding the transmission of radiance through the fog adapted to the heterogeneous dispersive environment. The distance map generated by approximate measurements and perspective projection was used in this paper. In the future, we aim to work on the automatic generation of this map using stereo-vision techniques or image analysis in two different weather conditions. Furthermore, another pivotal subject that we will treat soon is the estimation of the parameters of the radiation transmission model to develop an algorithm for enhancing visibility during fog.

Received on October 1, 2020

REFERENCES

1. S.G. Narasimhan, S.K. Nayar, *Vision and atmosphere*, IEEE Int. J. Comp. Vision, **48**, 3, pp. 233–254 (2002).
2. J.P. Oakley, B. L. Satherley, *Improving image quality in poor visibility conditions using a physical model for contrast degradation*, IEEE Trans. Image Process. **7**, pp. 167-179 (1998).
3. S.P. Narendra, L. Shyam, S.A. Kshitij, *A robust framework for visibility enhancement of foggy images*, Eng. Scie. and Technol., an Intl. J. **22**, 1, pp. 22–32 (2019).
4. G. Fan, T. Jin, X. Xiaoming, *Foggy scene rendering based on transmission map estimation*, Int. J. of Comp. Games Technol., Article ID 308629, (2014).
5. W. Xinhua, O. Jihong, W. Yi, L. Fei, Z. Guang, *Real-time vision through haze based on polarization imaging*, Applied Sciences, **9**, 1, p. 142 (2019).
6. K. Anshu, K. G. Amarjeet, *Analysis of atmospheric scattering from digital images using temporal polarized vision*, Intl. Re. J. of Eng. and Technol., **4**, 5, pp. 1275–1284 (2017).
7. M.L. Pieper, D. Manolakis, E. Truslow, J. Jacobson, A. Weisner, T. Cooley, *Wavelength calibration correction for ground radiance spectra in lwir hyperspectral imagery*, Proc. SPIE 10768, Imaging Spectrometry XXII: Applications, Sensors, and Processing, 18 September 2018.
8. K.J. Voss, S. Flora, *Spectral dependence of the seawater–air radiance transmission coefficient*, J. of Atmosph. and Oceanic Technol., **34**, pp. 1203–1205 (2017).
9. J.D. Pravin, S. Palanisamy, *New theoretical formulation for the determination of radiance transmittance at the water-air interface*, Optics Express 27102, **25**, No. 22, pp. 27086-27103 (2017).
10. ** *The Perlin noise math FAQ*. Available online: mzucker.github.io/html/perlin-noise-math-faq.html
11. J. Haber, M. Magnor, H.P. Seidel, *Physically based Simulation of twilight phenomena*, ACM Trans. on Graphics, **24**, 4, pp. 1-21 (2005).